# Evidence for a Light-Induced Degradation Mechanism at Elevated Temperatures in Commercial N-Type Silicon Heterojunction Solar Cells

*Brendan Wright, Chukwuka Madumelu, Anastasia Soeriyadi, Matthew Wright, and Brett Hallam**

The response of commercial n-type silicon heterojunction (SHJ) solar cells to illuminated annealing at temperatures between 75 and 180 °C is reported on. Although a slight increase in efficiency of 0.1% absolute occurs at 75 °C under 1 sun illumination after 20 h, annealing at higher temperatures (85–180 °C) results in significant degradation in cell performance, and only occurs in the presence of illumination. At 160 °C, a loss in $\eta$ up to 1% absolute is observed under 1 sun light soaking (LS) in as little as 2 min. Further illuminated annealing leads to a subsequent partial or full recovery of cell performance. At 160 °C, after an initial $V_{OC}$ degradation exceeding 10 mV within 3 min, a complete recovery is obtained after 60 min of illuminated annealing. The results indicate the potential presence of a light-induced degradation mechanism in n-type SHJ cells, suggesting care must be taken when using LS to improve efficiency. In addition, significant variability in the maximum extent of degradation indicates a high degree of cell-to-cell variation in expression of this degradation mechanism. The exact nature of the underlying defect mechanism(s) governing degradation and recovery dynamics remains uncertain and requires further studies.

Increasing interest in the development of next-generation silicon solar cell architectures has spurred research into a range of passivated contact designs, accomplishing carrier selectivity and surface passivation solely through the use of interfacial materials, in lieu of traditional diffused-junction based emitters. Silicon heterojunction (SHJ) solar cells are a leading example of this approach, currently holding the world record silicon solar conversion efficiency ($\eta$) at 26.7%, and as such have seen growing commercial interest in recent years.[1,2]

The SHJ architecture features an n-type crystalline silicon (c-Si) bulk wafer with hydrogenated amorphous silicon (a-Si:H)-based carrier-selective contacts; thin-film stacks deposited onto each surface of the c-Si wafer comprising a thin intrinsic interlayer (i-a-Si:H) coated with thicker doped layers ([p/n]-a-Si:H), subsequently capped with a transparent conducting oxide (TCO) film and finally metal contacts. The extremely low surface recombination afforded by this method of interfacial passivation commonly produces high open-circuit voltages ($V_{OC}$) upward of 730 mV at industry-scale production, consequently yielding commercially available cells with $\eta$ consistently exceeding 23%.[3]

A major advantage of the SHJ architecture is the inherently superior temperature coefficient, yielding a higher $V_{OC}$ at elevated temperatures when compared with alternate architectures featuring diffused emitters, arising primarily from improved surface passivation at the c-Si interface.[4] This has led to the preferential installation of high-efficiency modules incorporating SHJ cells in high temperatures and high irradiance environments, with average daily module temperatures as high as 50 °C (peak module temperatures exceeding 90 °C) and, providing as high as a 10% increase in power generation relative to conventional c-Si solar cells.[5–8]

The growing commercial interest in SHJ cells has motivated corresponding research into the long-term stability of these cell architectures under various operational conditions. The supposed degradation-free nature of the n-type bulk wafers typically used in these architectures is a primary motivation, with the desire to avoid well-known light-induced degradation mechanisms common to p-type wafers, including boron-oxygen defects and light- and elevated temperature-induced degradation (LeTID) behavior.[9–11] However, recent investigations indicate that n-type wafers may exhibit light-induced degradation effects after all, such as the recently identified LeTID effect.[12]

Further, while there exist reports indicating stability of the SHJ architecture, an increasing number of studies are reporting the observation of cell performance degradation, of unknown origin, during in-field operation.[5,13–15] An understanding of the underlying causal mechanisms responsible for this behavior is critically important if SHJ cells are to gain increasing marketshare.

Much of the studies to date have focused on the a-Si:H films directly as the source of cell performance instabilities, owing to

Dr. B. Wright, C. Madumelu, Dr. A. Soeriyadi, Dr. M. Wright, Dr. B. Hallam
School of Photovoltaic and Renewable Energy Engineering
UNSW
Sydney, Australia
E-mail: brett.hallam@unsw.edu.au

the well-known tendency of these materials to exhibit light-induced degradation via Staebler–Wronski (SW)-type defect mechanisms.[16–21] Many of these studies were, however, conducted on research samples rather than complete cells, leaving uncertainty as to the translation of observed behaviors into complete cells, featuring additional layer deposition and thermal processes.

Beyond incidental exposure during cell and module fabrication, some studies have indicated benefits to utilizing deliberate post-fabrication treatments on SHJ cells, including light soaking (LS) and dark annealing (DA) at elevated temperatures (≈150 °C), yielding an increase in $\eta$ up to 0.3% absolute after 30 h.[17,20,22] This process is however too slow for mass production, and the long-term persistence of these effects in operational cells is uncertain. Without a firm understanding of the underlying mechanisms responsible for cell performance enhancement, nor of the variability of final outcomes with relation to differences in cell fabrication, the effectiveness of such treatments remains controversial.

In this study we investigate the impact of illuminated annealing at temperatures between 75 °C and 180 °C on commercially sourced n-type SHJ cells. Although improvements can be observed at 160 °C, we identify the presence of a novel light-induced degradation mechanism at elevated temperatures, which is subsequently characterized in more detail via ex situ current–voltage (I–V) measurements.

To validate previous reports of SHJ cell efficiency enhancement during illuminated annealing, ex situ I–V measurements were carried out on cells as a function of exposure time. The results shown in **Figure 1** display SHJ cell performance variation during illuminated annealing at 75 °C under 1 sun equivalent illumination intensity: a) $\eta$, b) $V_{OC}$, and c) pseudo fill factor (pFF). Each plot displays the mean and standard deviation for a group of four equivalent cells as a function of exposure time. Both short-circuit current ($J_{SC}$) and series resistance ($R_S$) were found to be invariant over the studied exposure time, exhibiting values of $37.85 \pm 0.1 \, \mathrm{mA \, cm^{-2}}$ and $0.50 \pm 0.01 \, \Omega \, \mathrm{cm^{-2}}$ for $J_{SC}$ and $R_S$, respectively.

These results do indeed indicate an improvement in $\eta$ on the order of 0.1% absolute after 20 h for the studied SHJ cells, arising primarily from a 5 mV increase in $V_{OC}$. This behavior is comparable with that reported by Kobayashi et al, with a 0.2% increase in $\eta$ and 4 mV increase in $V_{OC}$ after illuminated annealing for 20 h.[20]
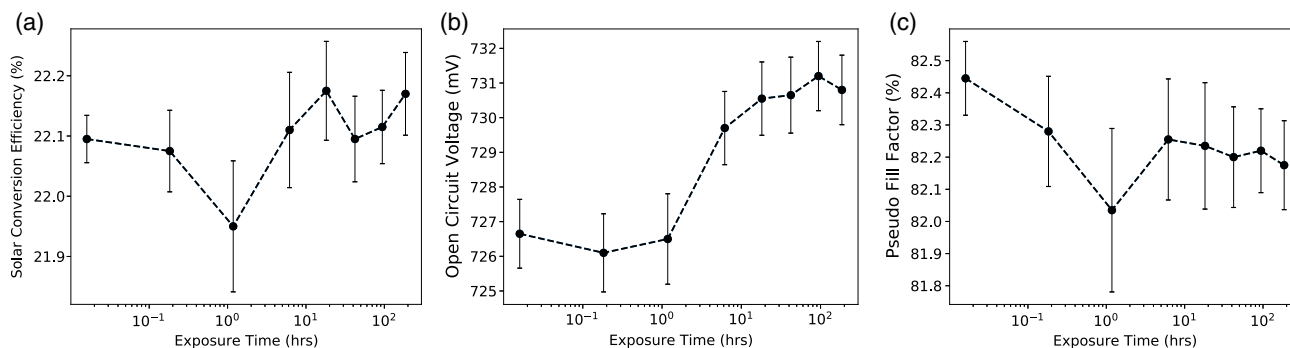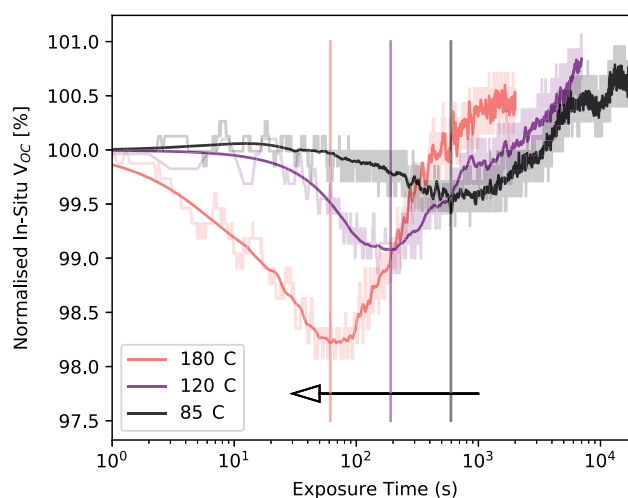


**Figure 2.** Normalized in situ open-circuit photovoltage transients for cells exposed to elevated temperatures from 85 °C up to 180 °C under 1 sun illumination. Solid vertical line overlain each transient indicate the point of maximum degradation extent, arrow indicating shift with increasing cell temperature.

To investigate the influence of increasing cell temperature on the kinetics of efficiency enhancement, in situ open-circuit photovoltage measurements were carried out. The results shown in **Figure 2** show in situ $V_{OC}$ transients (log$_{10}$-exposure time, normalized to the average initial $V_{OC}$ of 730 mV as measured ex situ prior to beginning cell processing) for cells under 1 sun illumination at elevated temperatures from 85 °C up to 180 °C, over an aggregate exposure time up to ≈5 h. Each $V_{OC}$ transient represents the smoothed response of a single cell during illuminated annealing.

The 85 °C transient exhibits a net increase in $V_{OC}$ similar to that observed in the 75 °C ex situ results shown in Figure 1, with the $V_{OC}$ observed to increase by 7 mV between 2 h and 5 h exposure time. However, it becomes clear that there is in fact an initial degradation phase prior to this improvement in $V_{OC}$, which at 85 °C is on the order of 2 mV. With increasing cell temperature this degradation becomes more prominent and reaches values as high as 14 mV at 180 °C.

To highlight the relative kinetics of the observed degradation, a solid vertical line is overlain each transient and indicates the



**Figure 1.** Solar cell performance variation during illuminated annealing at 75 °C under 1 sun equivalent illumination intensity: a) $\eta$, b) $V_{OC}$, and c) pFF. Each plot displays the mean and standard deviation for a group of four equivalent cells as a function of exposure time.

point of maximum $V_{OC}$ degradation extent, with an arrow indicating a shift to shorter exposure times with decreasing cell temperature. A clear dependency of $V_{OC}$ degradation and recovery kinetics on temperature is observed, with higher cell temperatures yielding a relative shift in degradation peak time from 700 s at 85 °C down to 70 s at 180 °C. Further, the relative maximum extent of $V_{OC}$ degradation also shows a strong temperature dependence, with the degradation at 180 °C exceeding the degradation at 85 °C by a factor of three.

Importantly, the final value of $V_{OC}$ still indicates an improvement over the initial value on the order of 4 mV, irrespective of the extent of initial degradation. Further, the higher relative cell temperatures do in fact accelerate the kinetics of this enhancement effect, with the 180 °C treatment reaching a net improvement within 10 min, over an order of magnitude faster than that of the 85 °C treatment.

The accuracy of in situ $V_{OC}$ measurement used in this study is limited to the order of ±2 mV, due to minor thermal variations during measurements, and the need for temperature correction to 25 °C equivalent for comparison. As such, ex situ I–V measurements were performed prior to and after 1 sun illuminated annealing for a total of 35 min at 180 °C, 125 mins at 120 °C, and 350 mins at 85 °C, each corresponding to the time at which measured in-situ $V_{OC}$ was observed to stabilize. The I–V results for these cells prior to processing exhibited average $\eta$ of 21.9 ± 0.1%, $V_{OC}$ of 729.5 ± 1.6 mV, and pFF of 82.7 ± 0.4%. After illuminated annealing, $\eta$ was found to be effectively equivalent to the preprocessed state at 21.9 ± 0.2%, whereas a minor increase in $V_{OC}$ to 730.1 ± 3.8 mV and decrease in pFF to 82.3 ± 0.7% was observed. Both the measured $J_{SC}$ and $R_S$ remained stable through processing, at 37 ± 0.1 mA cm$^{-2}$ and 0.59 ± 0.05 Ω cm$^2$, respectively.

The cell annealed at 85 °C exhibited the greatest net $V_{OC}$ increase of 3.1 mV, with a corresponding net improvement in $\eta$ of 0.19% absolute. The cell annealed at 180 °C, however, exhibited a net decrease in $V_{OC}$ of 0.8 mV and a net loss in $\eta$ of 0.2% absolute. These results indicate net $V_{OC}$ improvements lower than that implied from the in situ $V_{OC}$ results (Figure 2) and may be explained by additional degradation occurring during removal from elevated temperatures and cooling to room temperature prior to subsequent I–V measurements.

To further investigate the identified degradation behavior at elevated temperatures during illuminated annealing, which has not been previously reported for n-type SHJ cells to the best of our knowledge, detailed ex situ I–V measurements were carried out at an elevated temperature of 160 °C to study the degradation and recovery behavior. In addition, the impact of illumination versus DA is investigated, and a reference group of cells illuminated at room temperature is also included.

The results shown in **Figure 3** exhibit the primary solar cell performance instability at each of the three conditions: LS (1 sun equivalent illumination intensity) at room temperature (RT) (25 °C), DA at an elevated cell temperature of 160 °C (no illumination), and a combination of LS at 160 °C, all as a function of exposure time for each: a) $\eta$, b) $V_{OC}$, and c) pFF. Individual cell values are displayed (points), as well as box plots indicating mean and standard deviation of the five-cell groups and a time-averaged transient over exposure time (lines) to help guide the eye. In addition, no significant variation in $J_{SC}$ or $R_S$ was observed during exposure (not shown) at any of the above conditions, averaging 37.7 ± 0.1 mA cm$^{-2}$ and 0.55 ± 0.05 Ω cm$^2$ for $J_{SC}$ and $R_S$, respectively.

Interestingly, in contrast to both boron-oxygen and LeTID defects where $J_{SC}$ reduction is commonly observed, arising from increased bulk recombination, no such variation in $J_{SC}$ is observed in these cells under conditions that exhibit strong degradation and recovery behavior.[23,24]

The reference room temperature LS transients (dotted line in each plot of Figure 3) do not exhibit a significant change in either $\eta$ or $V_{OC}$ over the measured 15 min processing period (less than 0.2% absolute $\eta$ and 2.5 mV $V_{OC}$ at peak). The average pFF, however, does exhibit a gradual decline from the initial 83.3–82.5% after 15 min. A comparable reduction in pFF is also observed for the DA group beyond 5 min and is attributed to degradation in the form of increased charge carrier recombination arising from processing damage, including both manual handling and thermal cycling, inherent to the iterative ex situ measurement processes.

The cells exposed to elevated temperature without illumination (DA at 160 °C, dashed line in each plot of Figure 3) are observed to be more stable than that observed under illumination at the same temperature, exhibiting a relative improvement over the initial $\eta$ of 0.2% absolute within the first 2 min of exposure, with both $V_{OC}$ and pFF improving slightly.

The initial improvement is consistent with previously observed behaviors of the well-known recovery of reversible SW-type defects in the a-Si:H layers of each selective contact, typically observed when annealing in the dark for only a few
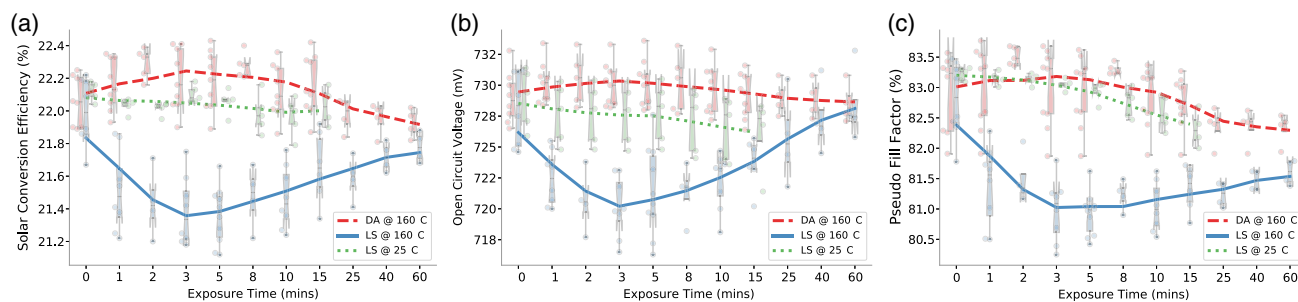


**Figure 3.** SHJ solar cell performance variation during exposure: a) $\eta$, b) $V_{OC}$, and c) pFF. Conditions as labelled: LS under 1 sun equivalent illumination intensity at either 25 or 160 °C; DA without light exposure at 160 °C. Individual cell values displayed (points), as well as box plots indicating mean and standard deviation of each five-cell group, and a time-averaged transient over exposure time (lines) to help guide the eye.

minutes at temperatures above 150 °C.[25] The initial state of SW defects (the fraction of recombination-active to dormant recombination-inactive states) is set at the time of i-a-Si layer deposition in the absence of any subsequent elevated temperature processing, as is the case for these plated-contact cells. Exposure of the cells to ambient light during initial cell characterization measurements (prior to any exposure to elevated temperatures) may also have been sufficient to activate SW defects, possibly accounting for the observed behavior.

Finally the addition of illumination at the very same elevated temperature (LS at 160 °C, solid line in each plot of Figure 3) produces strong and clearly observable degradation; reduction in both $V_{OC}$ and pFF is observed as soon as the cells are exposed to a combination of illumination and elevated temperature. The maximum extent of this degradation occurs prior to 4 min of illumination exposure, with an average loss of 10 mV in $V_{OC}$ and 2.0% absolute in pFF, yielding an average absolute loss in $\eta$ of 0.7% (peak individual cell loss exceeding 1.0%).

A subsequent recovery in $V_{OC}$ (and to a far lesser extent pFF) is observed beyond 5 min processing time, yielding an increase in $\eta$ of 0.5% absolute compared with that at the maximum degradation extent. For some cells this represents a net improvement in $V_{OC}$ up to 2 mV after 60 min of exposure time; however, pFF remains significantly reduced relative to the initial predegraded state, yielding an average of 0.2% absolute loss in $\eta$. It is important to note that the absence of any degradation with DA at the same temperature indicates that this is a light-induced degradation mechanism.

The observed kinetics and extent of $V_{OC}$ degradation and recovery behavior are also qualitatively in agreement with that observed for the in situ $V_{OC}$ results at 180 °C (Figure 2); the maximum extent of $V_{OC}$ degradation occurs on the order of 3 min exposure time, and a subsequent recovery in $V_{OC}$ approaches the initial value after 60 min.

Further testing of cells taken to the point of maximum degradation (5 min under 1 sun at 160 °C) exhibited a high degree of stability in this degraded state (maintained at room temperature without further light exposure for up to 4 weeks; less than 0.1% absolute variance in $\eta$; not shown), indicating that these changes to cell performance during exposure are effectively permanent, assuming no further exposure to illuminated annealing.

The variation in both $V_{OC}$ and pFF indicates that increased charge carrier recombination under illumination at elevated temperatures likely represents the primary mechanism by which the observed light-induced degradation manifests, a similar conclusion to that reached by Kobayashi et al.[20,22] It is also worth highlighting the high degree of variability in the maximum extent of $\eta$ and $V_{OC}$ reduction between individual cells. Although the standard deviation in $\eta$ of the initial state is less than 0.1% absolute, this increases to as much as 0.4% about the point of maximum degradation extent, indicating that there exists a high degree of cell-to-cell variation in the magnitude of the observed light-induced degradation mechanism, even for cells that appear equivalent prior to annealing.

The observed degradation mechanism appears to be a thermally activated process. It also appears likely that, at temperatures below 85 °C, the rate of the degradation process may simply be balanced (or exceeded) by the rate of the recovery process, and as such no net degradation has been observed.

In addition, as both degradation and recovery phases are observed, the underlying mechanism is unlikely to be a degradation of a-Si and may instead be related to a redistribution of defect density within the a-Si layers.[19]

We examined the response of commercial n-type SHJ solar cells to illuminated annealing at temperatures between 75 and 180 °C. A slight increase in $\eta$ of 0.1% absolute and in $V_{OC}$ of 5 mV is observed at 75 °C under 1 sun illumination after 20 h. This $V_{OC}$ enhancement can be accelerated by increasing annealing temperatures up to 160 °C, yielding a comparable improvement after 1 h, over an order of magnitude faster than that obtained at 75 °C. However, additional degradation in the form of pFF reduction at these higher temperatures results in a net loss in $\eta$ of 0.2% absolute.

Besides $V_{OC}$ and $\eta$ enhancement, we also observe a light-induced degradation mechanism when performing illuminated annealing at higher temperatures (85–180 °C), resulting in a significant degradation in both $V_{OC}$ and pFF, and consequently $\eta$, arising from increased charge carrier recombination. At 160 °C, up to a 1.0,% absolute loss in $\eta$ can be observed under 1 sun LS in as little as 2 min. Importantly, no such instability is observed at identical temperature without illumination, confirming that this is in fact a light-induced behavior. Further illuminated annealing can lead to a subsequent partial or full recovery of cell performance. At 160 °C, even after an initial $V_{OC}$ degradation exceeding 10 mV within 3 min, a complete recovery is obtained after 60 min of illuminated annealing. However, the majority of pFF degradation that occurs during processing is not recovered, even when complete recovery of $V_{OC}$ is observed.

The observation of a recovery implies that this behavior is not simply a degradation of a-Si layers. In addition, both the kinetics and maximum degradation extent are found to increase at increasing illuminated annealing temperatures, indicating that this may be a thermally activated process related to defect redistribution within the a-Si layers. We also note significant variability in the maximum extent of $\eta$ and $V_{OC}$ reduction between individual cells, indicating that there exists a high degree of cell-to-cell variation in the magnitude of the observed light-induced degradation mechanism. This may arise from differences in a-Si layer defect density distribution between cells, set during the a-Si deposition process, where larger relative defect densities could result in a greater maximum extent of degradation.

Importantly, if accidental exposure to light and elevated temperature occurs sufficient to drive the cells into a maximally degraded state, the effective loss in cell $\eta$ can be commercially significant. This result stands in contrast to previous reports suggesting that deliberate LS of SHJ cells is necessarily beneficial.[22] Further investigations are needed into the stability of the degraded state under various illumination intensities and elevated temperatures relevant to in-field operation. In addition, future studies into the modulation of this defect using illuminated annealing should seek to understand at what combination of illumination intensity and temperature does the observed effects start to become commercially relevant and to understand whether all SHJ cells are prone to this behavior, as well as to develop an improved understanding of the underlying causal mechanism(s).

## Experimental Section

A batch of commercially sourced n-type SHJ cells (6 inch, bifacial) were used for this study, with measured average $V_{OC}$ and $\eta$ of $729 \pm 2$ mV and $22.1 \pm 0.1\%$, respectively, for a group of 30 cells. The structure of these cells featured an n-type mono (Cz) silicon wafer, with selective contact stacks at each interface comprising: a thin i-a-Si:H passivation layer and (p/n)-a-Si:H carrier selective layer, finished with a TCO film and plated metal (Cu and Sn) contacts.

LS at elevated temperatures (160 °C) was conducted using a LS stage featuring uniform area halogen lamps for illumination, calibrated to 1 sun equivalent power density, with the cells at open-circuit conditions. The cells were positioned on an electronically controlled hotplate with an independent temperature probe at the wafer edge. In addition, DA was conducted using the same set-up in the absence of illumination. LS at room temperature (25 °C) was performed using a separate set-up featuring light-emitting diode bulbs for illumination, with intensity below 0.2 kW m$^{-2}$ to avoid heating the cells.

At each increment of exposure time, the cells were removed from illumination and elevated temperature (allowed to cool to room temperature where required) for calibrated $I–V$ measurements (reverse/forward bias sweeps under AM1.5G solar spectrum equivalent illumination) using a solar simulator (LOANA by pv-tools GmbH), each cell affixed via vacuum to a temperature-controlled chuck maintained at 25 °C during measurement. In addition to a standard $I–V$ sweep, a Suns-Voc measurement was also carried out to obtain an $I–V$ response without the influence of $R_s$ and thereby calculate pFF.

On separate samples, in situ $V_{oc}$ measurements were carried out using a custom voltage probe station (a continuous data acquisition rate of 10 points per second), mounted to the aforementioned LS stage. The cell rear surface contacted the hotplate surface and additionally served as the anode contact, whereas a separate voltage pin was placed in contact with a busbar region on the front surface. Voltage transients were recorded as the cell entered the elevated temperature and illumination environment. Reference $I–V$ measurements were also carried out at room temperature using the solar simulator (LOANA) prior to, and after LS or dark annealing.

## Conflict of Interest

The authors declare no conflict of interest.

## Keywords

illuminated annealing, light-induced degradations, n-type wafers, silicon heterojunctions

[1] T. G. Allen, J. Bullock, X. Yang, A. Javey, S. D. Wolf, *Nat. Energy* **2019**, *4*, 914.

[2] K. Yoshikawa, H. Kawasaki, W. Yoshida, T. Irie, K. Konishi, K. Nakano, T. Uto, D. Adachi, M. Kanematsu, H. Uzu, K. Yamamoto, *Nat. Energy* **2017**, *2*, 17032.

[3] J. Zhao, M. Konig, A. Wissen, V. Breus, D. Decker, M. Fritzsche, M. Schorch, H. J. Nonnenmacher, M. Leonhardt, T. Große, J. Hausmann, A. Waltinger, D. Landgraf, S. Burkhardt, H. Mehlich, E. Vetter, F. Schitthelm, Y. Yao, T. Söderström, A. Richter, D. Habermann, S. Leu, *IEEE 44th Photovoltaic Specialist Conf.*, IEEE, Washington, DC **2017**, pp. 1752–1754.

[4] M. Taguchi, E. Maruyama, M. Tanaka, *Jpn. J. Appl. Phys.* **2008**, *47*, 814.

[5] A. Abdallah, D. Martinez, B. Figgis, O. E. Daif, *Renewable Energy* **2016**, *97*, 860.

[6] J. K. Kaldellis, M. Kapsali, K. A. Kavadias, *Renewable Energy* **2014**, *66*, 612.

[7] A. M. Ciesla, J. I. Bilbao, C. E. Chan, D. N. R. Payne, D. Chen, M. Kim, S. R. Wenham, B. J. Hallam, *IEEE J. Photovoltaics* **2020**, *10*, 28.

[8] J. Kurnik, M. Jankovec, K. Brecl, M. Topic, *Sol. Energy Mater. Sol. Cells* **2011**, *95*, 373.

[9] F. Kersten, P. Engelhart, H.-C. Ploigt, A. Stekolnikov, T. Lindner, F. Stenzel, M. Bartzsch, A. Szpeth, K. Petter, J. Heitmann, J. W. Muller, *Sol. Energy Mater. Sol. Cells* **2015**, *142*, 83.

[10] W. Fischer, H. Pschunder, *Proc. 10th Institute of Electrical and Electronics Engineers Photovoltaic Specialists Conf.*, IEEE, New York, NY **1973**, p. 404.

[11] K. Ramspeck, S. Zimmermann, H. Nagel, A. Metz, Y. Gassenbauer, B. Birkmann, A. Seidl, S. S. Ag, S. Solar, W. Gmbh, in *27th Eur. Photovolt. Sol. Energy Conf. Exhib.*, WIP Renewable Energies, München, **2012**, p. 861.

[12] D. Chen, P. G. Hamer, M. Kim, T. H. Fung, G. Bourret-Sicotte, S. Liu, C. E. Chan, A. Ciesla, R. Chen, M. D. Abbott, B. J. Hallam, S. R. Wenham, *Sol. Energy Mater. Sol. Cells* **2018**, *185*, 174.

[13] J. Karas, A. Sinha, V. S. P. Buddha, F. Li, F. Moghadam, G. TamizhMani, S. Bowden, A. Augusto, *IEEE J. Photovolt.* **2020**, *10*, 153.

[14] D. C. Jordan, C. Deline, S. Johnston, S. R. Rummel, B. Sekulic, P. Hacke, S. R. Kurtz, K. O. Davis, E. J. Schneller, X. Sun, M. A. Alam, R. A. Sinton, *IEEE J. Photovolt.* **2018**, *8*, 177.

[15] D. C. Jordan, S. R. Kurtz, K. VanSant, J. Newmiller, *Prog. Photovoltaics Res. Appl.* **2016**, *24*, 978.

[16] M. Stutzmann, W. B. Jackson, C. C. Tsai, *Phys. Rev. B* **1985**, *32*, 23.

[17] E. M. El Mhamdi, J. Holovsky, B. Demaurex, C. Ballif, S. De Wolf, *Appl. Phys. Lett.* **2014**, *104*, 252108.

[18] S. De Wolf, S. Olibet, C. Ballif, *J. Appl. Phys. Lett.* **2008**, *93*, 032101.

[19] P. Mahtani, R. Varache, B. Jovet, C. Longeaud, J.-P. Kleider, N. P. Kherani, *J. Appl. Phys.* **2013**, *114*, 124503.

[20] E. Kobayashi, S. De Wolf, J. Levrat, G. Christmann, A. Descoeudres, S. Nicolay, M. Despeisse, Y. Watabe, C. Ballif, *Appl. Phys. Lett.* **2016**, *109*, 153503.

[21] S. Bernardini, M. I. Bertoni, *Phys. Status Solidi A*, **2019**, *216*, 1800705.

[22] E. Kobayashi, S. De Wolf, J. Levrat, A. Descoeudres, M. Despeisse, F.-J. Haug, C. Ballif, *Sol. Energy Mater. Sol. Cells* **2017**, *173*, 43.

[23] B. J. Hallam, P. G. Hamer, S. Wang, L. Song, N. Nampalli, M. D. Abbott, C. E. Chan, D. Lu, A. M. Wenham, L. Mai, N. Borojevic, A. Li, D. Chen, M. Y. Kim, A. Azmi, S. Wenham, *Energy Proc.* **2015**, *77*, 799.

[24] B. Sopori, P. Basnyat, S. Devayajanam, S. Shet, V. Mehta, J. Binns, J. Appel, *38th IEEE Photovoltaic Specialists Conf.*, IEEE, Austin, TX **2011**, pp. 001115–001120.

[25] J. Kakalios, R. A. Street, W. B. Jackson, *Phys. Rev. Lett.* **1987**, *59*, 1037.